Evaluating the Effectiveness of Emerging Geophysical Methods to Characterize AFFF-Impacted Contaminant Source Areas

Presenter: Samuel Falzone *(Rutgers University, Newark, NJ)*

Co-Authors: Kristina Keating, Lee Slater *(Rutgers University, Newark, NJ)*

Charles Schaefer *(CDM Smith, Inc., Edison, NJ)*

Aqueous Film Forming Foam (AFFF)

Effective fire suppressant

Polyfluoroalkyl Substances (PFAS) form within contaminant source area

Emerging contaminant, especially at military bases

Fire Drill using AFFF

Polyfluoroalkyl Substances (PFAS)

Complex ionic properties (anionic, cationic and zwitterionic)

Exhibit strong interaction with solid-phase organic material

Sorption likely for cationic and zwitterionic constituents (*Deeb et al.*, 2017)

Association with the soil surface opens the door to using geophysics for characterization

Fluorinated Tail

Hydrophilic Head

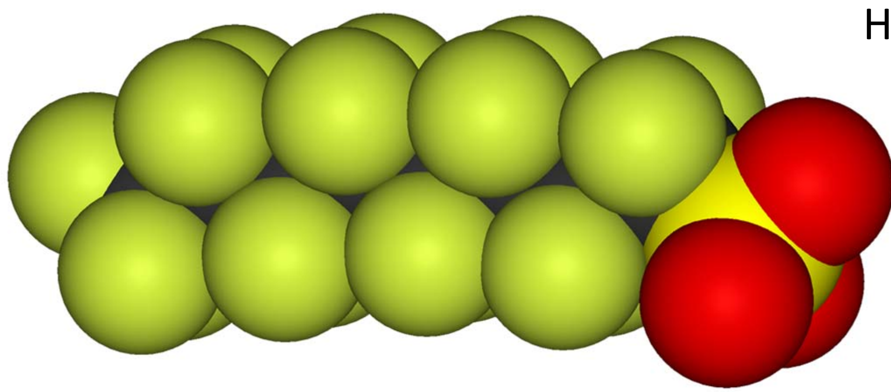

Objective

Determine sensitivity of geophysical methods to PFAS contamination

Explore strengths and limitations of methods through benchtop experiments

Limited scope feasibility study aimed at steering future funding

ERT Survey of the Hanford Site

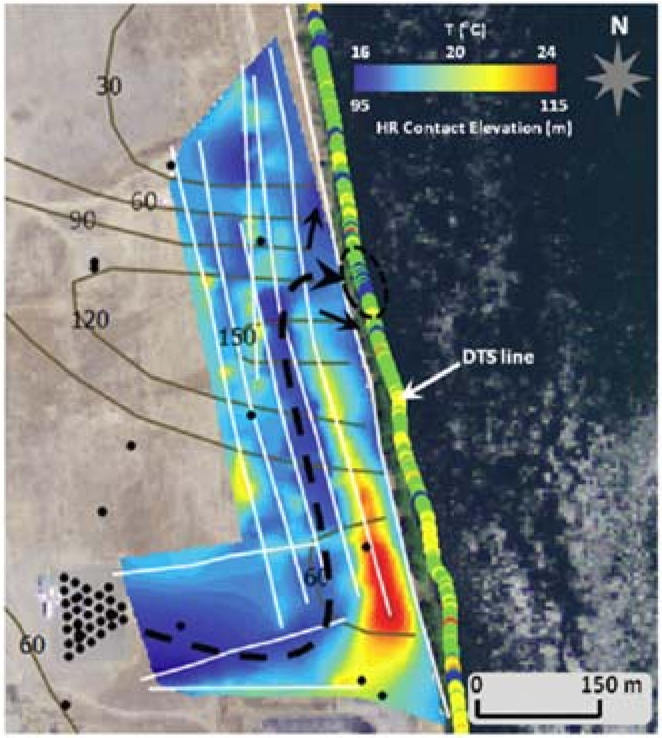

Modified from Mwakanyamale et al. 2012

Geophysical Method

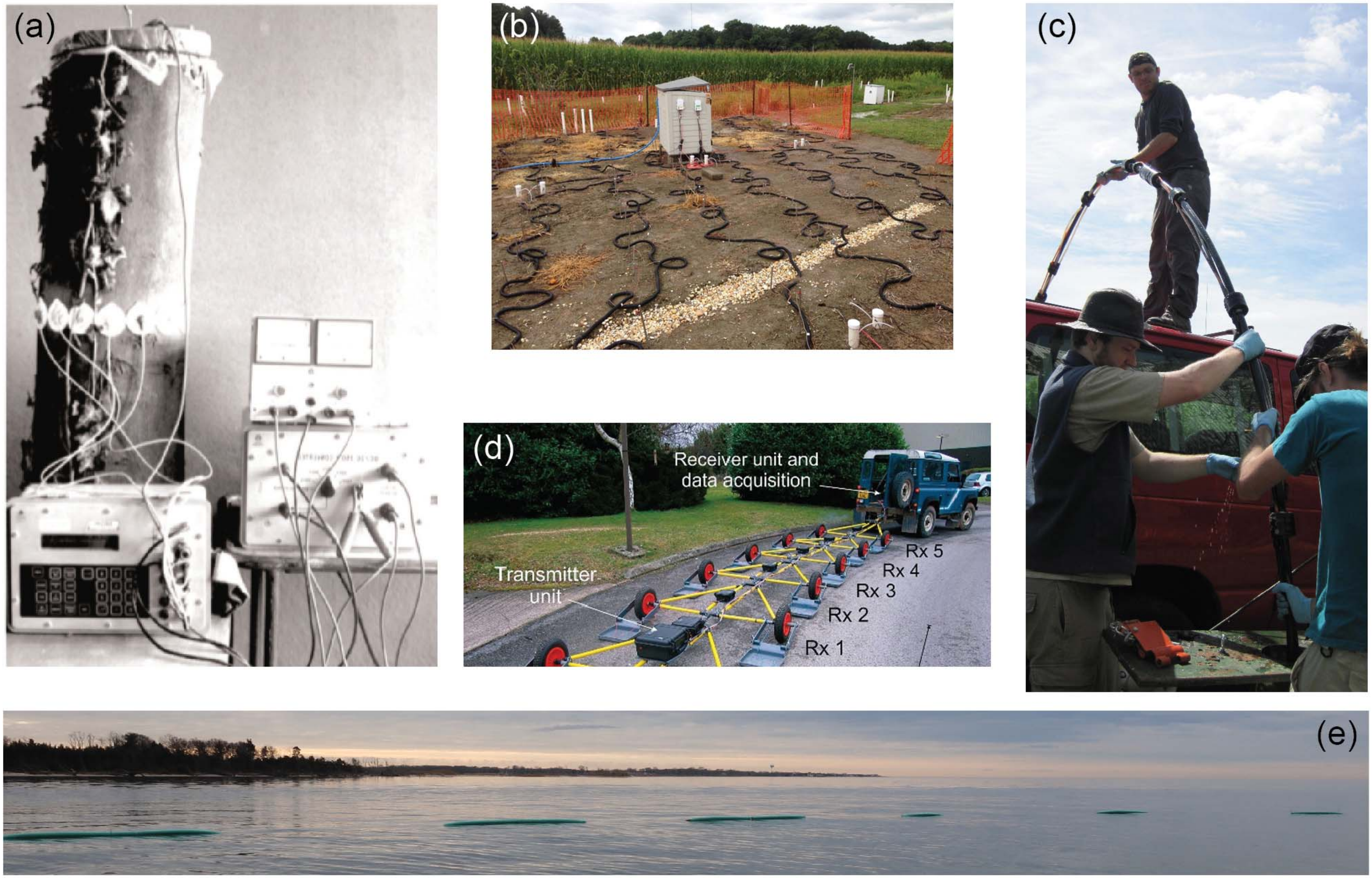

Modified from Falzone et al. 2018, Al Hagrey 2006, Kuras et al. 2007

Geophysical Method

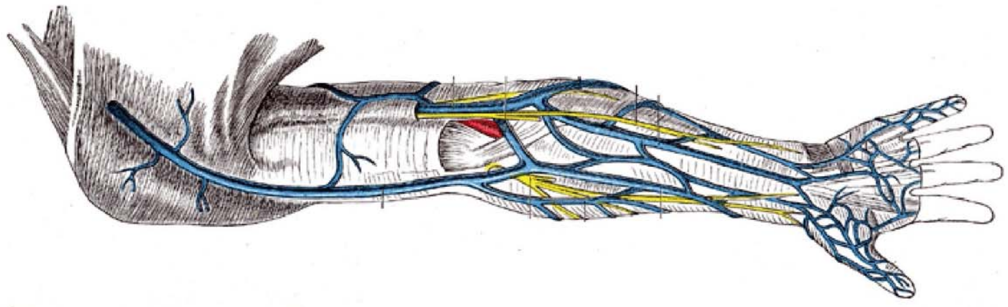

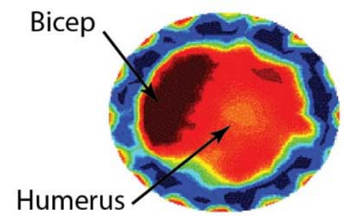

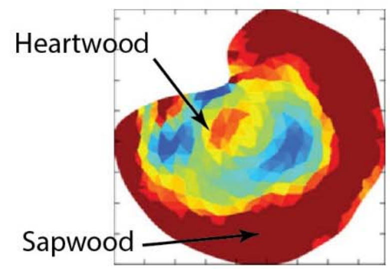

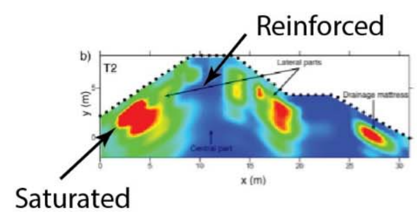

Modified from Falzone et al. 2018

Geophysical Method

Surface Tomographic Survey of Earthen Dam

Established methods are non-unique and interpretable

Electrical resistivity tomography of a reconstructed levee

Grout injection and ballast areas are visible as contrasting resistive structures

Water saturated areas are evident as less resistive areas

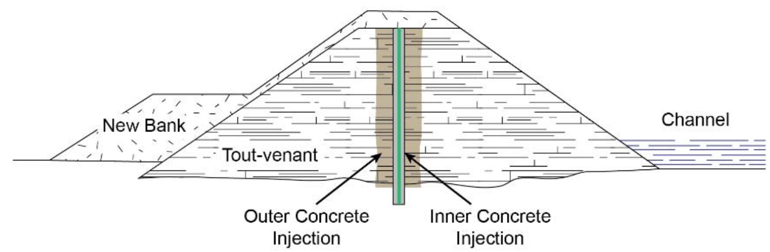

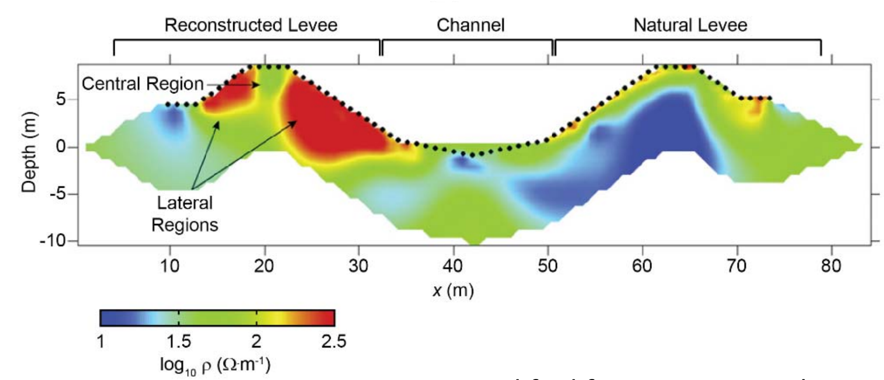

Modified from Busato et al. 2016

Modified from Busato et al. 2016

Geophysical Method

3D Surface Survey

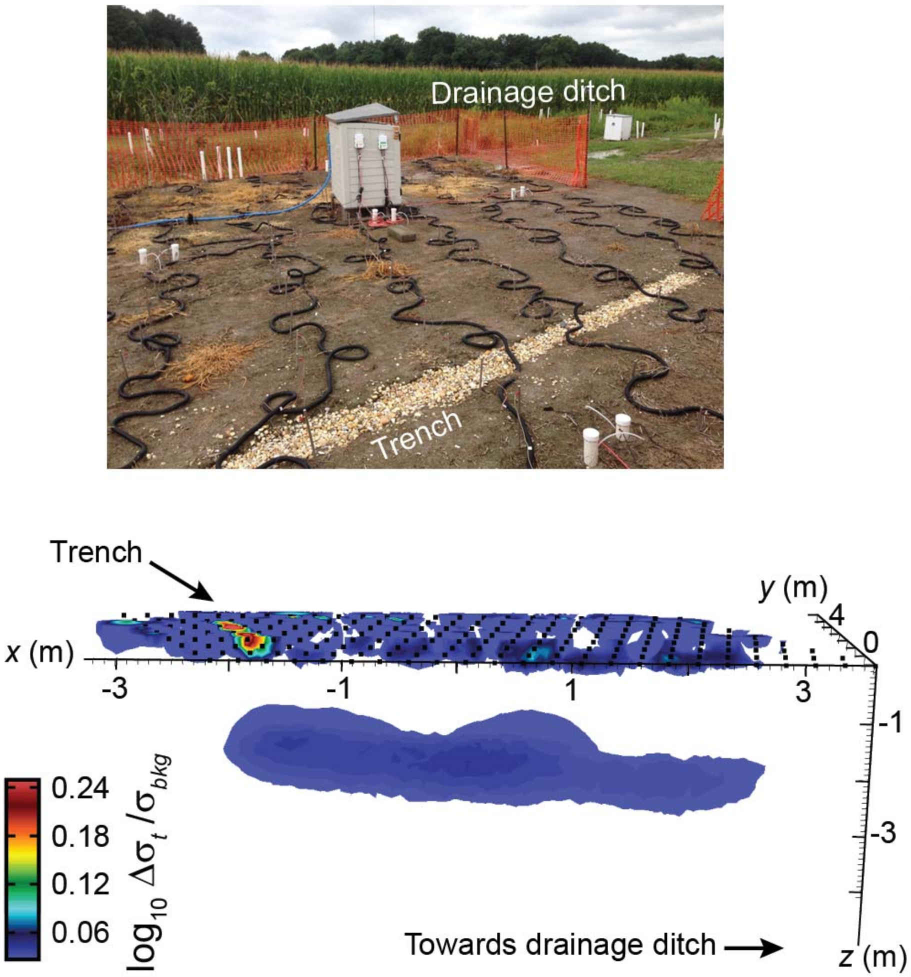

Modified from Falzone et al. 2018

Borehole Survey

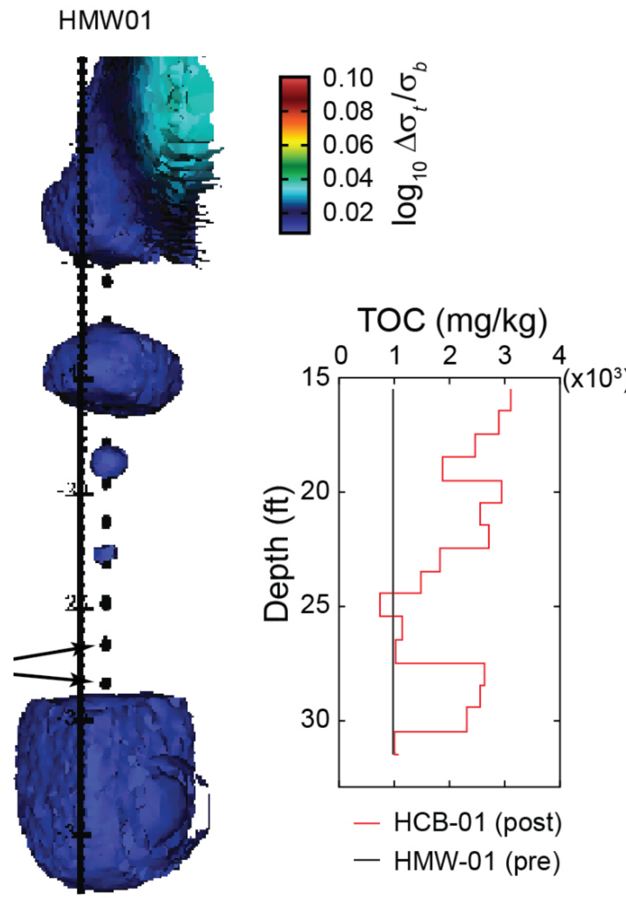

Modified from Falzone et al. 2018

Emerging Geophysical Methods

Nuclear Magnetic Resonance (NMR)

Directly sensitive to water, saturation and porosity

Sensitive to pore scale environments, including surface area and surface mineralogy

Cranial MRI

Modified from Pasieka/Science Photo Library

Induced Polarization (IP)

Like ERT, but with added sensitivity to surface electrical properties

Can be adapted for borehole, surface, time-lapse imaging

IP Image of a Tree Trunk

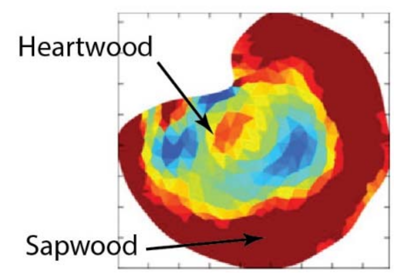

Modified from Falzone et al. 2018

Emerging Geophysical Methods

Infiltration Test from Walsh et al., 2014

Modified from SAVSARP, Tucson Water, AZ

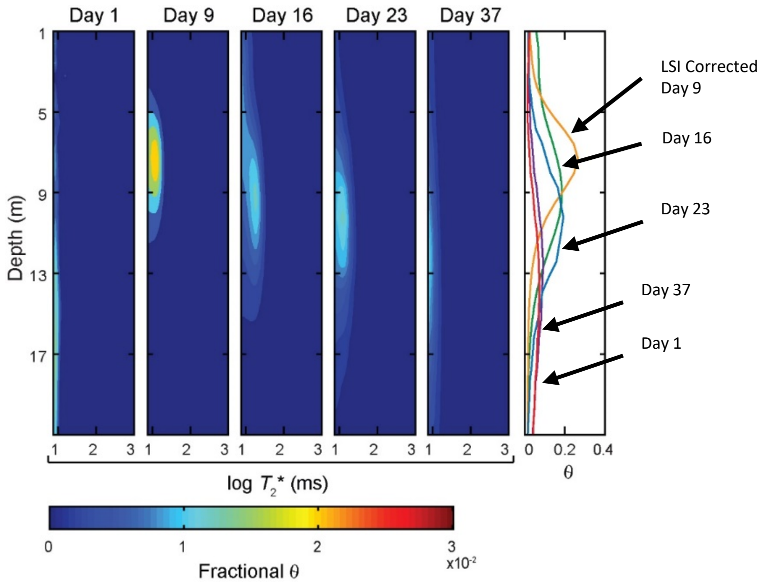

Modified from Falzone and Keating 2016

Recent technological development has increased the practicality of using these methods

New instrumentation includes borehole, surface, and advanced laboratory instrumentation

Emerging methods better suited for characterizing fate and transport of contaminants

Induced Polarization

Measures the complex conductivity of porous media

Capable of differentiating between several conductive properties of porous media

Sensitive to surface mineralogical changes and pore size

Benchtop IP Measurements

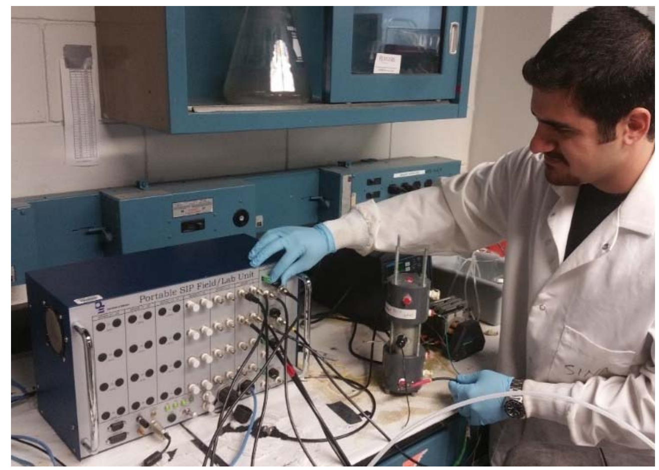

Induced Polarization

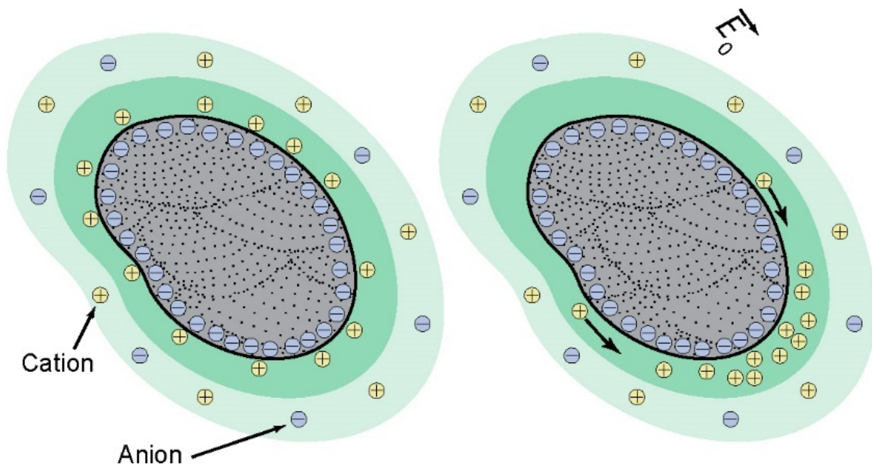

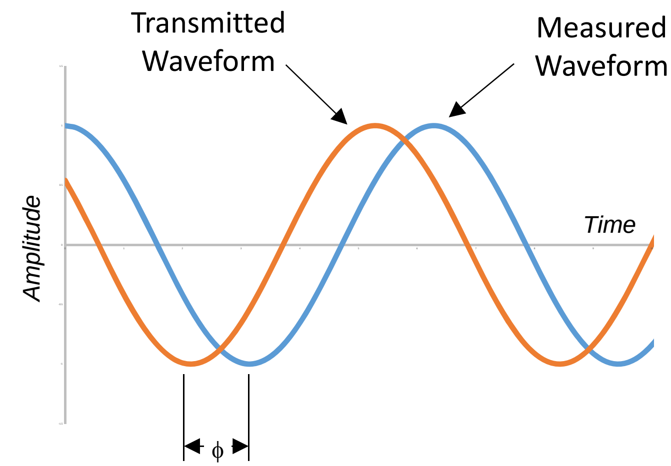

Measures in the frequency domain

Capable of obtaining the complex resistivity

$$\sigma' = \frac{1}{F}\sigma_{fluid} + \sigma_{surf}$$

Weller et al. (2013)

$$\sigma'' = 0.042\sigma_{surf}$$

IP Phase Spectrum

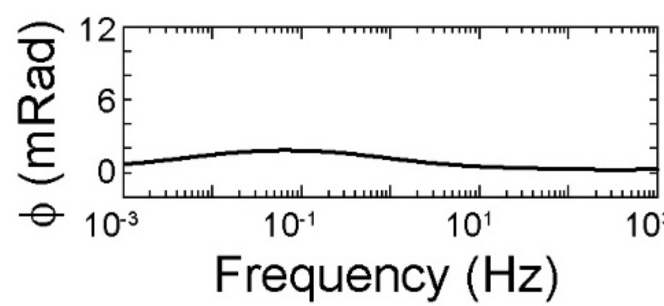

Induced Polarization

Several studies have outlined the close link between the IP response and sorption

Hao et al. (2016) demonstrated a close link between the σ'' and ^{22}Na tracer injections

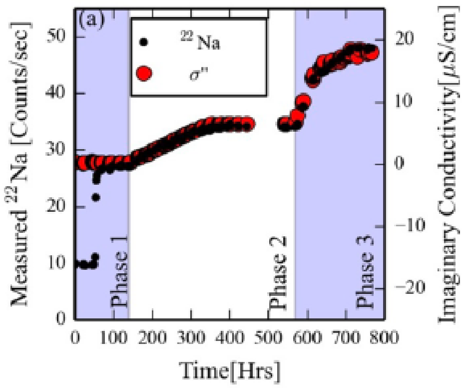

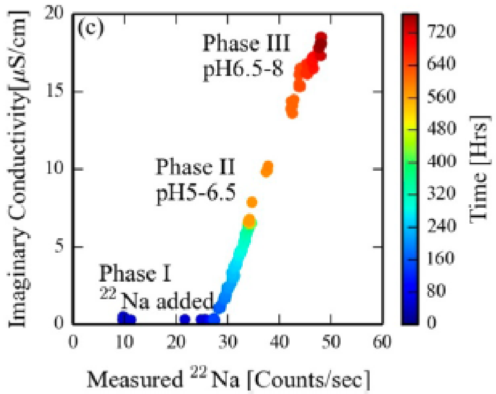

Modified from Hao et al. 2016

Nuclear Magnetic Resonance

Directly measures the presence of hydrogen in water within porous media

Sensitive to pore size and surface mineralogy

Also capable of determining spatial distribution of water within porous media (1D imaging)

NMR Benchtop Instrument

Nuclear Magnetic Resonance

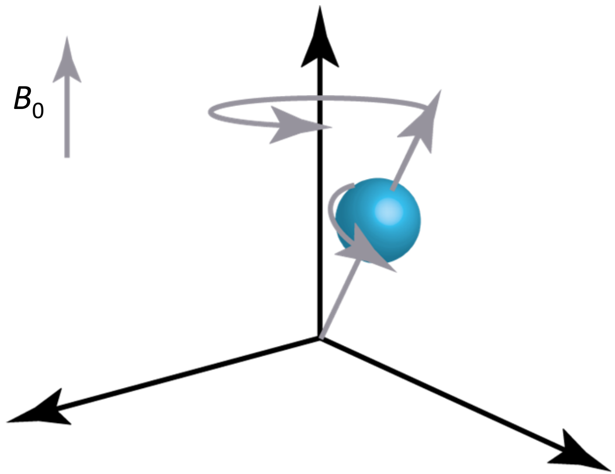

$$f_0 = \frac{\gamma |B_0|}{2\pi}$$

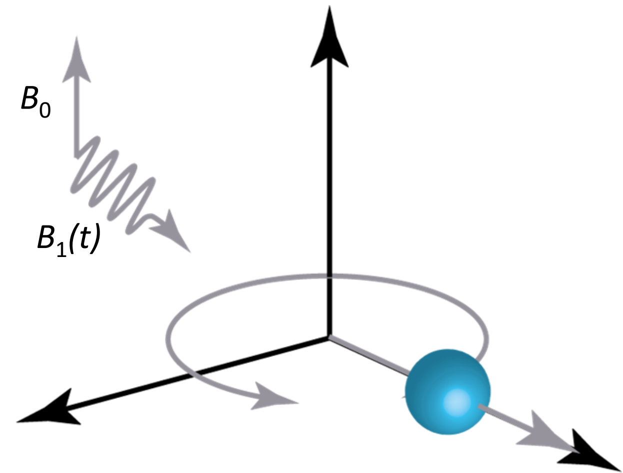

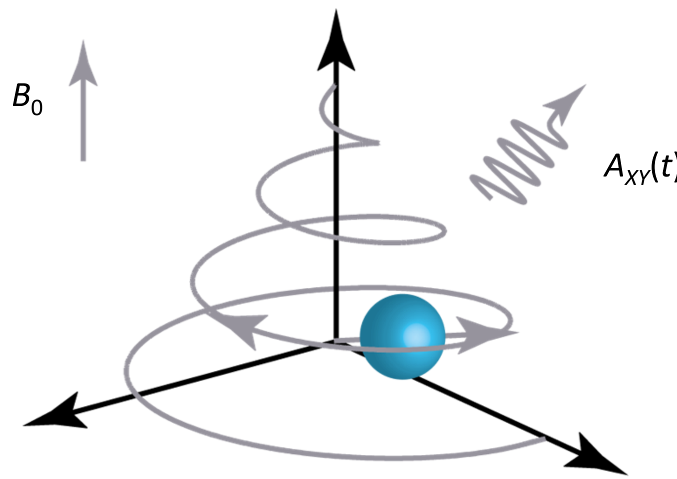

f_0 = Larmour frequency
B_0 = Static magnetic field intensity
γ = gyromagnetic ratio of hydrogen
t is time
$A_{XY}(t)$ is measured signal
A_i is i^{th} signal component
T_{2i} is i^{th} relaxation time
A_0 is initial signal magnitude

Nuclear Magnetic Resonance

Proton/Paramagnetic Coupling

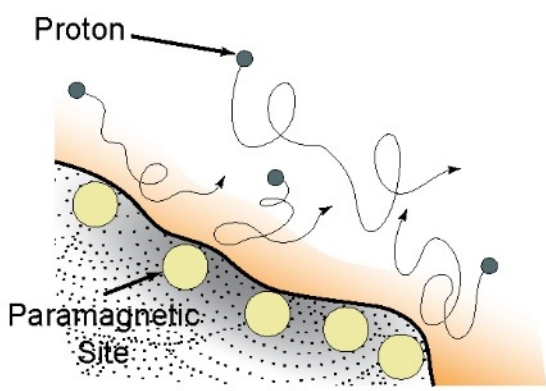

$$\sum_i A_i = A_0 \approx \theta$$

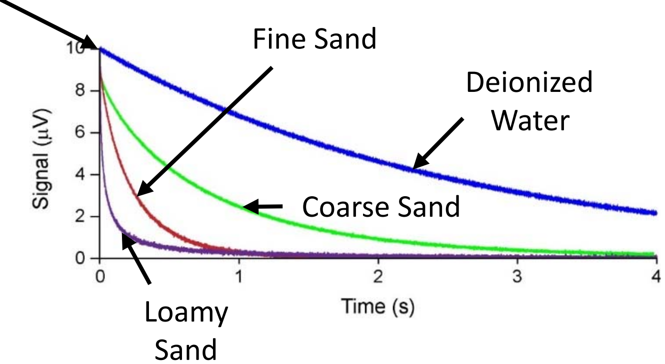

$$A_{XY}(t) = \sum_i A_i e^{\left(\frac{-t}{T_{2i}}\right)}$$

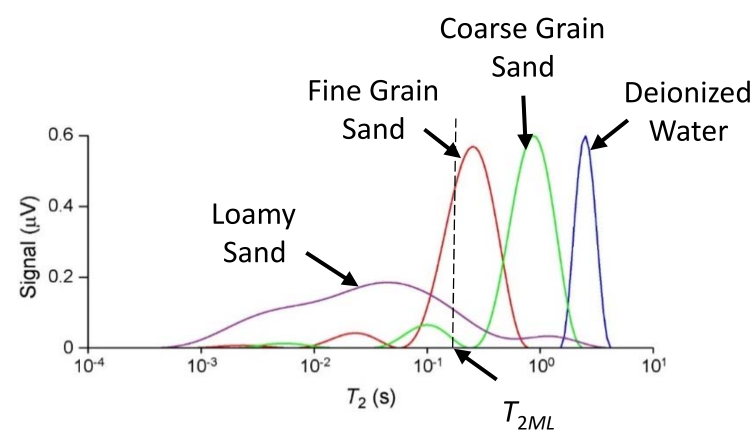

Nuclear Magnetic Resonance

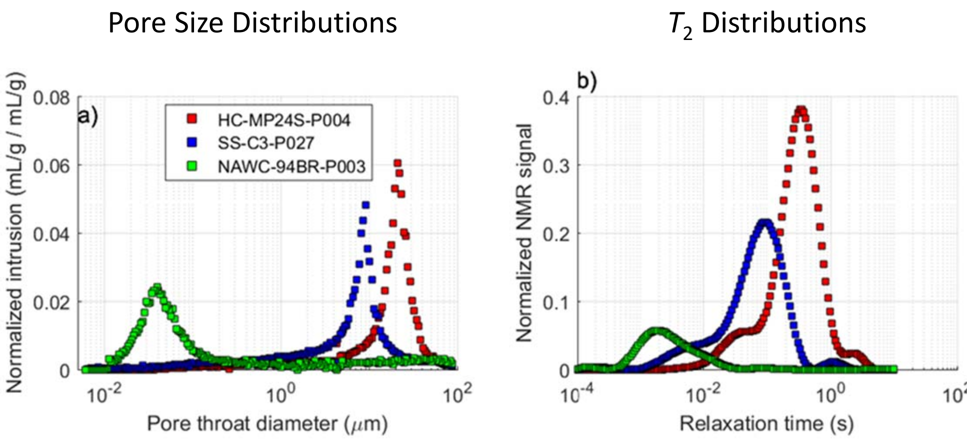

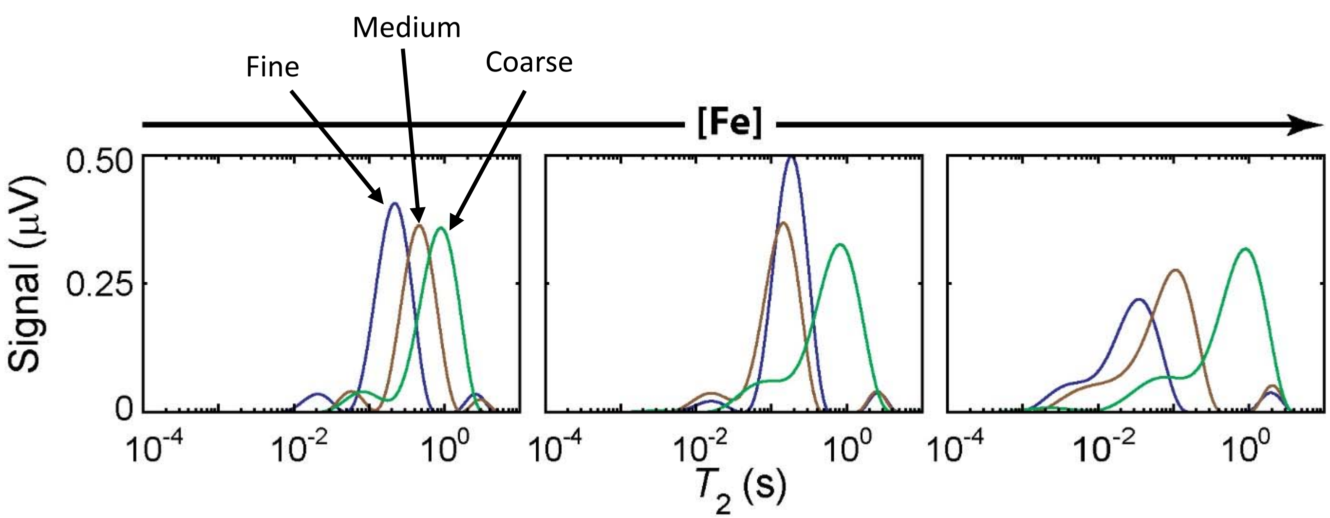

Modified from Keating and Falzone 2013

Column Experiment

<u>Procedure</u>

Synthetic soils made from clay/sand/peat/hematite analyzed in column experiments

Columns were exposed to AFFF contaminated groundwater

NMR and IP measurements taken for 8 days following contamination

Soil Packed Columns

Benchtop IP

Benchtop NMR

Potential NMR Response from PFASs

Augmented
Proton/Paramagnetic Coupling

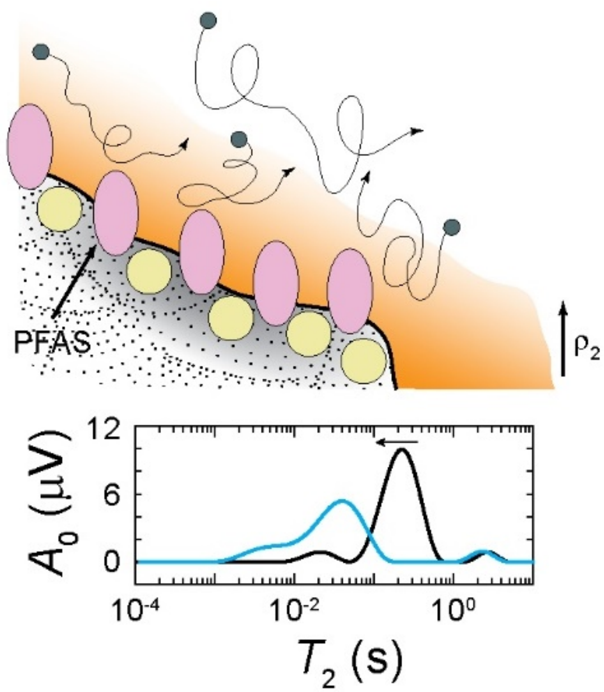

Diminished
Proton/Paramagnetic Coupling

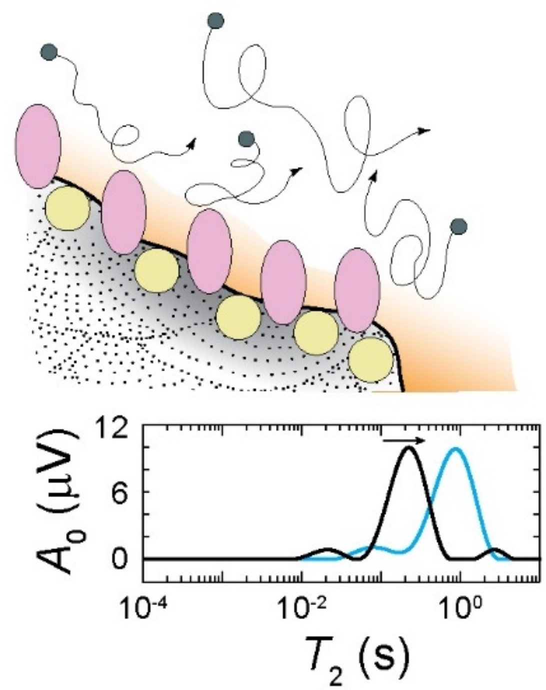

Potential IP Response from PFASs

Augmented Polarization

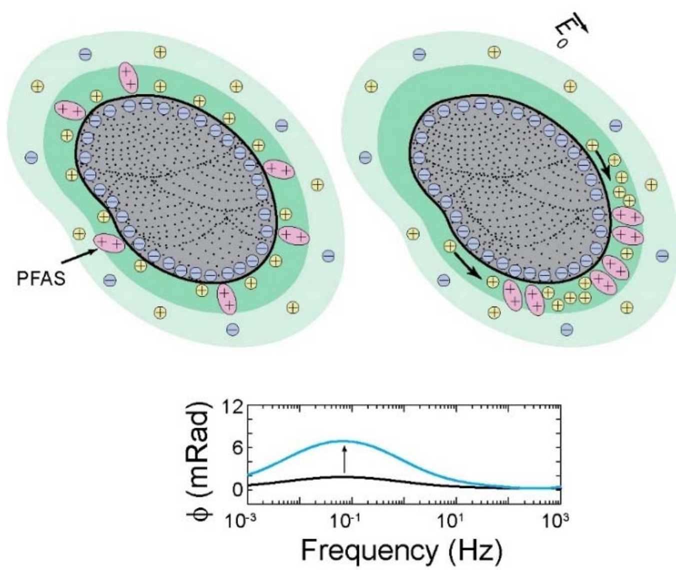

Diminished Polarization

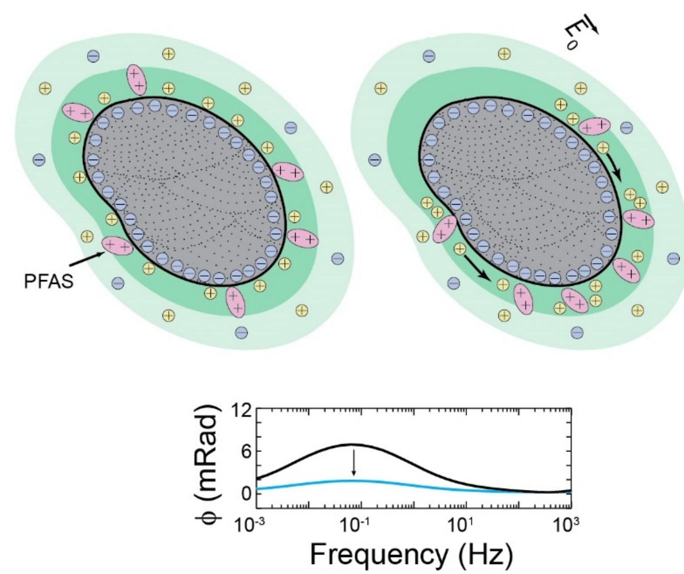

IP Data

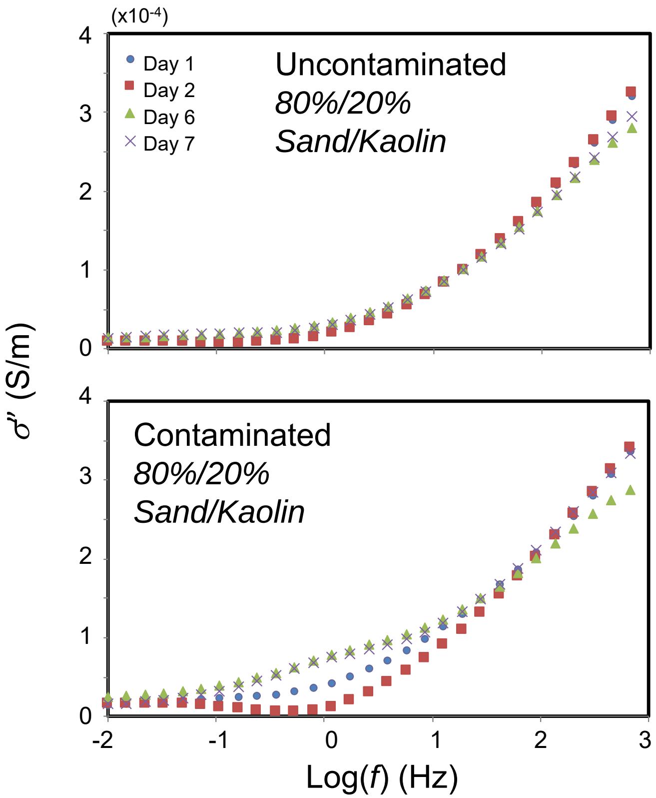

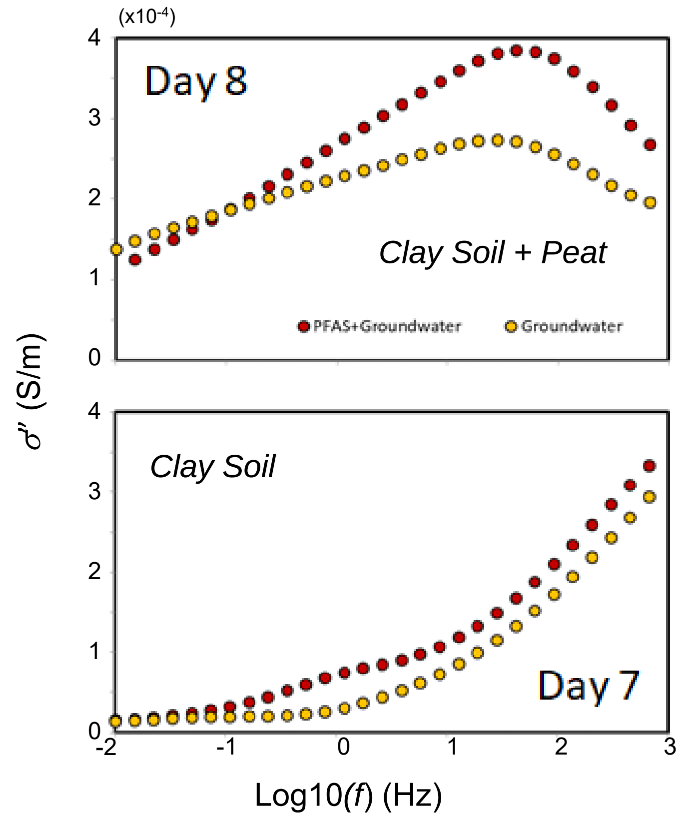

Uncontaminated samples exhibited constant σ'' through out experiment

Contaminated samples exhibited noticeable increase in σ'' over same period

NMR Data

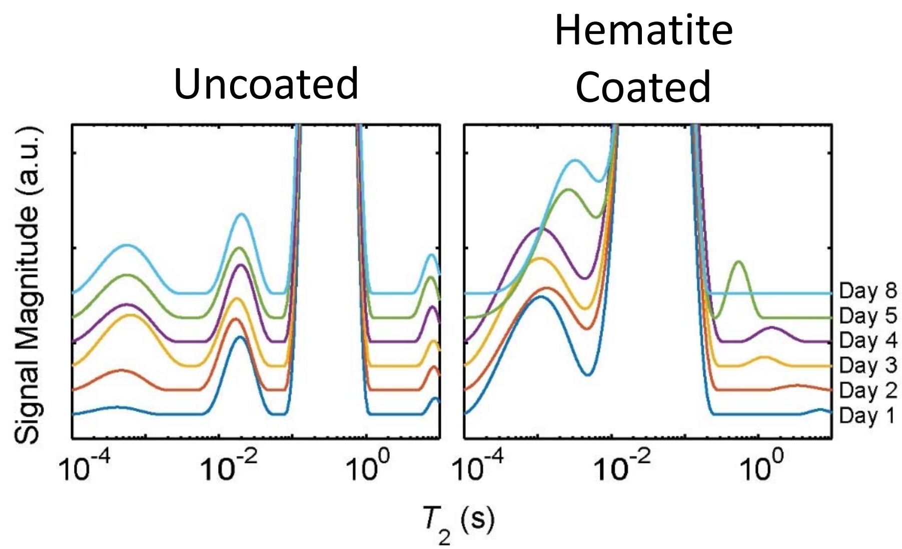

Uncontaminated sample exhibited constant T_2 distribution over 8 days

Contaminated sample exhibited shift in T_2 distribution to longer relaxation times over same time period

Conclusions

Observed response in both NMR and IP data over 8 days following contamination

Similar observations are absent from uncontaminated columns

Response seems to be dependent on soil types (i.e. presence of clay, iron minerals, organic material)

IP response appears to be due to increased polarization within the double layer

NMR response appears to be due to masking of proton-paramagnetic coupling at the pore surface

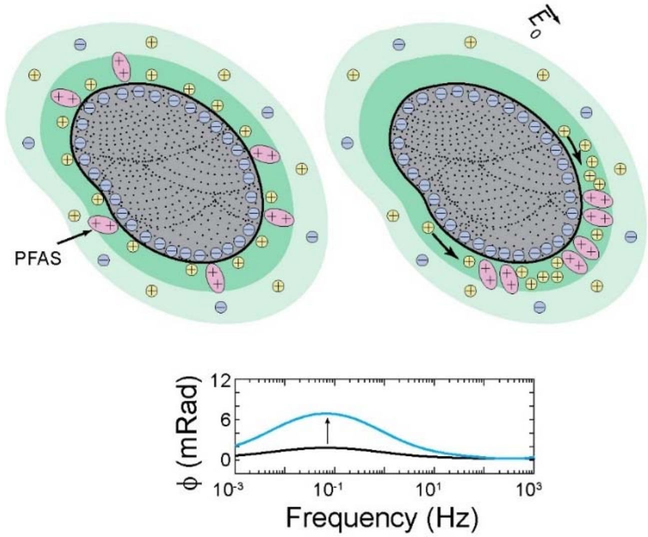

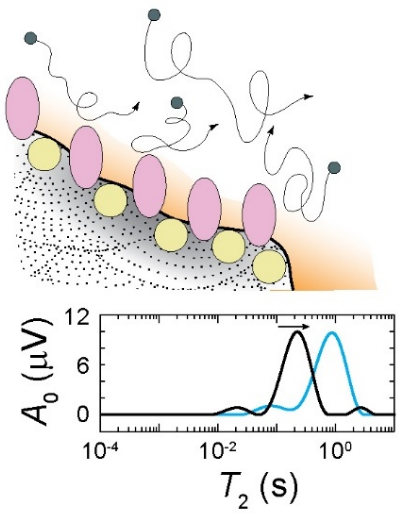

Citations

Al Hagrey, S. (2016). Electrical resistivity imaging of tree trunks. Near Surf. Geophys. 4(3), 179–187.

Busato, L., J. Boaga, L. Peruzzo, M. Himi, S. Cola, S. Bersan and G. Cassiani. (2016). Combined geophysical surveys for the characterization of a reconstructed river embankment. Eng. Geol. 211, 74–84.

Deeb, R., J. Field, E. Hawley and C. Higgins. (2017). Perfluoroalkyl and Polyfluoroalkyl Substances (PFASs). EnviroWiki

Falzone, S. and K. Keating. (2016). Algorithms for removing surface water signals from surface NMR infiltration surveys. Geophys. 81(4). WB97–WB107.

Falzone, S., J. Robinson, and L. Slater. (2018). Characterization and monitoring of porous media with electrical imaging. TIPM. (Special Issue).

Hao, Na, S.M.J. Moysey, B.A. Powell, and D. Ntarlagiannis. (2016). Comparison of the surface ion density of silica gel evaluated via spectral induced polarization versus acid–base titration. Journal of Appl. Geophys. 135, 427-435.

Keating, K. and S. Falzone (2013) Relating NMR relaxation time distributions to pore size distributions for unconsolidated sands. Geophys. 78(6). E365–E377.

Kuras, O., P.I. Meldrum, D. Beamish, R.D. Oglivy and D. Lala. (2007). Capacitive resistivity imaging with towed arrays. JEEG. 12, 267–279.

Mwakanyamale, K., F.D. Lewis and L.D. Slater. (2013). Statistical mapping of zones of focused groundwater/surface-water exchange using fiber-optic distributed temperature sensing. WRR. 49. 1-6. DOI:10.1002/wrcr.20458.

Walsh, D.O., E.D. Grunewald, P. Turner, A. Hinnell and T.P.A. Ferré. (2014) Surface NMR instrumentation and methods for detecting and characterizing water in the vadose zone. NSG. 12(2). 271–284.

Weller, A., L. Slater, S. Nordsiek and D. Ntarlagiannis. (2010). On the estimation of specific surface per unit pore volume from induced polarization: a robust empirical relation fits multiple data sets. Geophys. 75(4), WA105–SA112.